Archives of Mechanics • Archiwum Mechaniki Stosowanej • 31, 5, pp. 723–739, Warszawa 1979

Electrical characterization of transversely isotropic sands

Y. F. DAFALIAS and K. ARULANANDAN (DAVIS)

THE FORMATION factor F, defined as the ratio of the conductivity of the pore fluid which saturates a sand aggregate to the conductivity of the mixture, is shown theoretically to depend on the basic features of the sand structure. Analytical expressions are derived relating the formation factor to the porosity and properly defined parameters associated with the shape and orientation of particles for transversely isotropic sands. The dependence on the particles orientation is the reason why F assumes different values if measured along different directions of anisotropic sand samples. The derived expressions are used in order to predict the formation factor in different directions and porosities, by independently obtaining the values of the shape and orientation parameters from thin section studies of sands. Satisfactory agreement between the predicted and electrically measured values of F confirms the validity of the developed theory and proves the capability of F to characterize the sand structure, especially its feature associated with transversely isotropic symmetries most commonly encountered in practice.

Wykazano teoretycznie, że czynnik formacji F, zdefiniowany jako stosunek przewodności elektrycznej płynu porowego, który nasyca agregat piaskowy, do przewodności mieszaniny, zależy od podstawowych cech struktury piasku. Wyprowadzono wyrażenia analityczne wiążące czynnik formacji z porowatością i odpowiednio zdefiniowanymi parametrami związanymi z kształtem i orientacją cząsteczek dla piasków poprzecznie izotropowych. Zależność od orientacji cząsteczek sprawia, że F przyjmuje różne wartości przy pomiarach anizotropowych próbek piasku wzdłuż różnych kierunków. Wyprowadzone zależności zostały wykorzystane do przewidywania wartości czynnika formacji dla różnych kierunków i porowatości przez niezależne określanie wartości parametrów kształtu i orientacji z badania cienkich warstw piasku. Zadowalająca zgodność pomiędzy przewidywanymi i elektrycznie zmierzonymi wartościami F potwierdza słuszność opracowanej teorii i potwierdza przydatność F jako parametru charakteryzującego strukturę piasku, a szczególnie jego cechy związane z poprzecznie izotropowymi symetriami najczęściej spotykanymi w praktyce.

Теоретически показано, что фактор формации F, определенный как отношение электропроводимости пористой жидкости, которая насыщает песчаный агрегат, к проводимости смеси, зависит от основных свойств структуры песка. Выведены аналитические выражения, связывающие фактор формации с пористостью и с соответственно определенными параметрами, связанными с формой и ориентацией частиц для песков поперечно изотропных. Зависимость от ориентации частиц приводит к тому, что F принимает разные значения при измерениях анизотропных образцов песка вдоль разных направлений. Выведенные зависимости использованы для предсказания значений фактора формации для разных направлений и пористости путем независимого определения значений параметров формы и ориентации из исследования тонких слоев песка. Удовлетворительное совпадение между предсказанными и электрически измеренными значениями F подтверждает правильность разработанной теории и подтверждает значение F как параметра, характеризующего структуру песка, а особенно его свойства, связанные с поперечно изотропными симметриями наиболее часто встречаемыми на практике.

1. Introduction

SAND masses are in general anisotropic in both natural deposits and laboratory prepared samples mainly as a result of preferred orientation of the sand grains. Thin sections studies [11, 12] confirm a particular kind of anisotropy most commonly encountered, that of transverse isotropy characterized by a direction of rotational and reflectional symmetry of the sand structure, called the axis of transverse isotropy. The transverse isotropy has an important effect on the mechanical properties of sand such as friction angle, deformation characteristics, liquefaction, etc., as shown theoretically and experimentally in [2, 11, 12, 13, 14, 21, 22].

Any index used to characterize sands must take into account the basic features of the sand structure, namely porosity, size, shape, and orientation of particles. The most commonly used index, the relative density D_r, by definition does not depend on the orientation of particles and therefore cannot successfully be correlated with mechanical properties depending on anisotropy. For example, samples of the same sand prepared at the same relative density by different methods reflecting different orientation of particles, exhibited substantially different liquefaction and deformation behavior as shown by MITCHELL *et al.* [11].

A new index which has been shown experimentally to depend on the porosity, particle shape and size distribution and the direction of measurement is the formation factor F [3, 5, 6, 9, 20] defined as the ratio of the conductivity of the electrolyte which saturates a particulate medium with non-conductive particles to the conductivity of the mixture [ARCHIE [1]]. F does not depend on the conductivity of the electrolyte because a change of the latter changes proportionally the mixture conductivity, thus F remains constant. This is not true if the particles are conductive. In a recent study by ARULANANDAN and KUTTER [3] different values of F were measured along the vertical and horizontal directions of transversely isotropic sand samples, the vertical direction being the axis of transverse isotropy; subsequently the ratio of these values together with relative density was successfully correlated to the liquefaction behavior. The underlying reason for which F assumes different values if measured along different directions is the orientation of particles which changes the value of the mixture conductivity with direction for anisotropic sands.

The objective of this paper is to prove theoretically the directional dependence of F on porosity, particles' shape and orientation for transversely isotropic sands, and confirm the validity of the theory by comparing predicted to experimentally measured values of F. The theoretical proof of dependence of F on porosity and shape only, dates back to MAXWELL's fundamental work on spherical particles [7] followed by numerous works, a detailed account of which is given by MEREDITH and TOBIAS [10]. In a recent work by ARULANANDAN and DAFALIAS [23] the dependence of F on the orientation is studied for the case where all particles are identically oriented, but clearly this does not reflect realistically the multi-orientation character of a sand aggregate. DAFALIAS and ARULANANDAN [24] have considered the most general case of orientation by introducing appropriate probability density functions, but no prediction of F was possible.

Here closed-form analytical expressions are derived theoretically on the basis of the electromagnetic theory, relating the formation factor, the porosity, a shape factor S depending on the axial ratio R of the sand particles and an orientation factor P_θ depending on the orientation distribution of the particles' long axes with respect to the direction of transverse isotropy. Upper and lower bounds on quantities entering the above relations are established theoretically. The values of S and P_θ can be obtained independently from thin section studies for Monterey '0' sand and used in connection with the derived relations to predict the values of F along different directions for samples prepared by different methods at different porosities. The comparison with experimentally measured values of F is very satisfactory for most cases.

2. Transverse isotropy of sands

In mechanics a material is said to exhibit certain symmetries if its constitutive relations remain invariant under a certain group of orthogonal transformations of the coordinates of the reference configuration. Granular media can develop such symmetries as a result of the orientation of the solid particles. The invariance of their constitutive relations is therefore a direct reflection of symmetries characterizing the granular structure, hence it is equivalent to talk about structural invariance or structural symmetries.

Sand masses, both in natural deposits or laboratory prepared samples, are characterized mainly by two kinds of symmetries, isotropy and transverse isotropy. In isotropic sands the particles' orientation is statistically the same with respect to any axis of an arbitrarily chosen Cartesian coordinate system, therefore invariance is preserved under the full group of orthogonal transformations. Transversely isotropic sands are characterized by a definite direction commonly called the axis of rotational and reflectional symmetries, and is used as one of the coordinate axes. The statistical orientation of the particles is rotationally symmetric with respect to this axis, hence structural symmetry (and invariance of constitutive relations) is preserved under those orthogonal transformations of the coordinates which imply rotation around this axis and reflections with respect to planes containing the axis. In natural deposits the axis coincides with the direction which characterizes the sedimentation process, e.g. gravity, direction of flow, etc. In samples prepared in the laboratory by different methods like pluviation, tamping, vibration, etc. the axis coincides with the vertical direction associated with the sample preparation.

The transverse isotropy of the sand structure has been proved by direct observation of the particles' orientation. ODA [12, 13, 14] and MITCHELL *et al.* [11] offer a comprehensive study of the sand structure by the method of thin sections and the effect of particles' orientation on strength and liquefaction properties. In their investigation cylindrical samples were prepared by different methods and subsequently impregnated by resin. With the cylindrical axis being the vertical one, thin section were cut along the vertical and horizontal directions and the histograms of the particles' long axis orientations were obtained. The histograms associated with the horizontal sections indicated a random orientation of the long axes, thus proving the rotational and reflectional symmetries of the sand structure with respect to vertical axis. This was further supported by the fact that histograms associated with two perpendicular to each other vertical thin sections (i.e. containing the vertical axis) were statistically the same. Of course the degree of particles' orientation with respect to the vertical direction varies with porosity and method of preparation for the same sand. This is illustrated by the histograms of vertical sections shown in Figs. 2 and 1 for Monterey '0' sand at porosities 0.38 ($D_r = 80\%$)

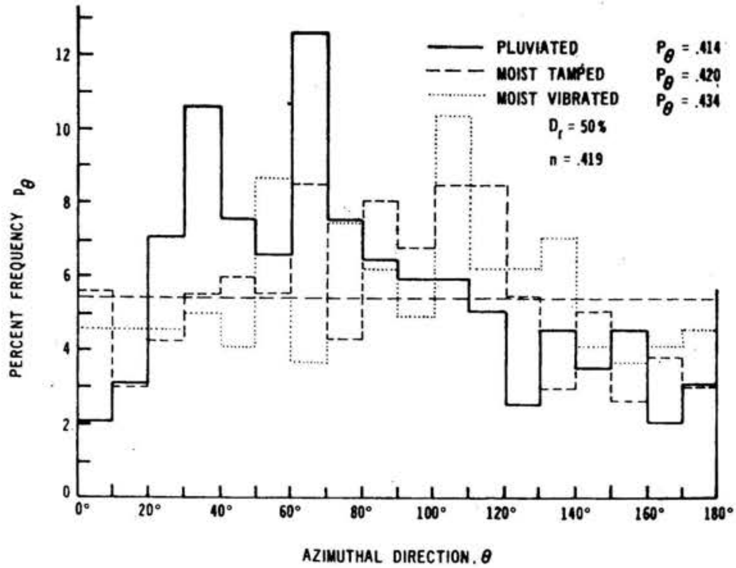

FIG. 1. Histograms of particle long axis orientations for samples of Monterey '0' sand prepared to 50% relative density by different methods (After MITCHELL *et al.* [11]).

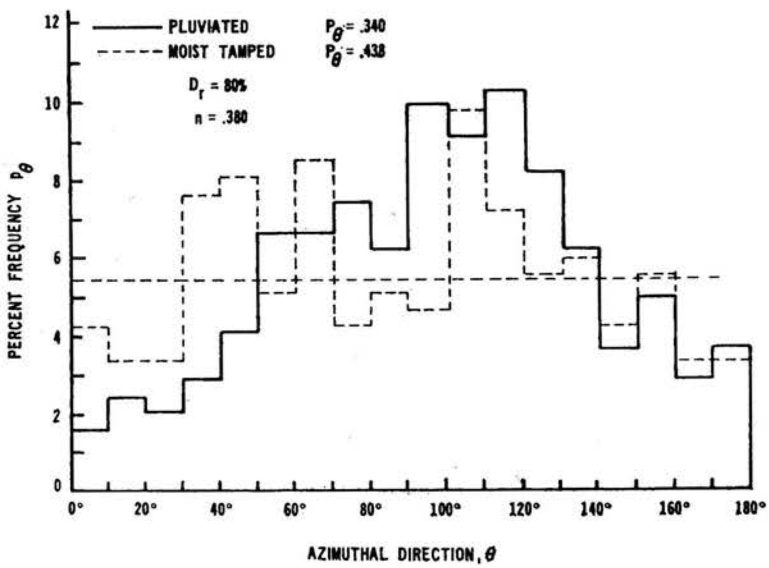

FIG. 2. Histograms of particle long axis orientations for samples of Monterey '0' sand prepared to 80% relative density by different methods (After MITCHELL *et al.* [11]).

and 0.419 ($D_r = 50\%$) respectively, as obtained by MITCHELL *et al.* [11]. The horizontal coordinate represents the azimuthal angle (or direction) θ between the long axis of a particle and the vertical direction. The vertical coordinate represents the percent frequency p_θ of particles with long axes inclined by θ with respect to the vertical. It is apparent from the histograms that the tendency for more horizontal orientation increases from moist vibrated, to moits tamped to pluviated samples; this was proved to substantially affect the liquefaction behavior, with the liquefaction resistance decreasing in the same order [11]. The orientation also changes with porosity as comparison between Figs. 1 and 2 reveals. A more detailed elabotraion of the orientation in terms of the formation factor is subsequently given.

3. The formation factor as a function of porosity, particles shape and orientation

3.1. General theory

A sand grain will be modelled as a prolate spheroid of axial ratio $R = b/a \leqslant 1$, with a and b the long and short semiaxes, respectively. The following analysis holds true also for oblate spheroids with $R = b/a \geqslant 1$. Consider such a non-conductive spheroid embedded in a electrolyte medium (water for soil mechanics) of conductivity k_e. If n is the porosity, the volume of the spheroid is 1-n, and its orientation is defined by the azimuthal angle θ formed by the semiaxis $OA = a$ with a direction OV, Fig. 3a. A potential dif-

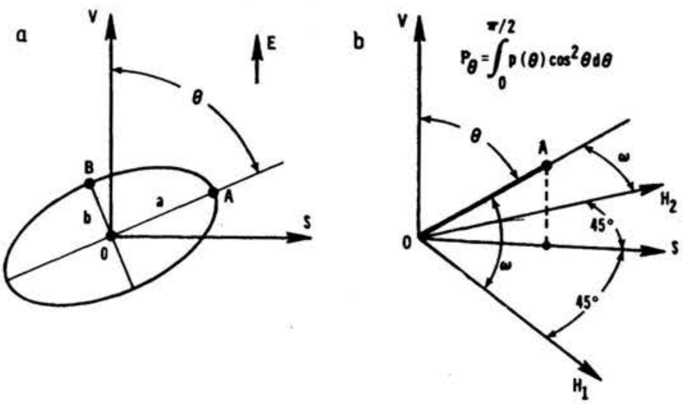

FIG. 3. Schematic illustration of particle's orientation in a transversely isotropic sand aggregate.

ference U yields a unidirectional electric field E along the direction OV before the insertion of the spheroid. After the insertion, the electric field for the space outside (denoted by a plus sign) and inside (denoted by a minus sign) the spheroid along the direction OV can be found by standard methods requiring the solution of the Laplace equation for the potential U in confocal elliptic coordinates subjected to appropriate boundary conditions, STRATTON [15]. After certain numerical simplifications possible for a spheroid and taking the ratio of the dielectric constant of sand to that of water approximately equal to zero, the solution for a very dilute dispersion yields for the electric field along OV

$$E^+ \simeq E, \qquad E^- = Ef_\theta, \tag{3.1}$$

$$(3.2)\qquad f_\theta = \frac{1}{1-S}\left(1-\frac{3S-1}{2S}\cos^2\theta\right),$$

$$(3.3)\qquad S = \frac{1}{2(1-R^2)}\left[\frac{R^2}{2\sqrt{1-R^2}}\ln\frac{1-\sqrt{1-R^2}}{1+\sqrt{1-R^2}}+1\right],\quad 0\leqslant R\leqslant 1,$$

$$(3.4)\qquad S = \frac{1}{2(R^2-1)}\left[\frac{R^2}{\sqrt{1-R^2}}\tan^{-1}\sqrt{R^2-1}-1\right],\quad 1\leqslant R,$$

where the quantity S is called the shape factor, depending only on the value of the axial ratio R.

Following FRICKE [6] and using Eqs. (3.1) and (3.2), the following two volume average equations can be written for the potential U and the total electric current (Ohm's law) recalling that the spheroid is non-conductive:

$$(3.5)\qquad \begin{aligned} U &= \int_+ E^+dx\,dA+\int_- E^-dx\,dA = (n+(1-n)f_\theta)\,E,\\ k_mU &= k_e\int_+ E^+dx\,dA = nk_eE, \end{aligned}$$

where k_m denotes the conductivity of the mixture and dx, dA represent line and area elements parallel and perpendicular respectively to the direction OV. Elimination of U, E from Eq. (3.5) yields finally for the formation factor F_θ the expression

$$(3.6)\qquad F_\theta = \frac{k_e}{k_m} = 1+\frac{1-n}{n}f_\theta.$$

Observe from Eq. $(3.5)_2$ that by changing k_e a proportional change of k_m takes place leaving F_θ constant. This would not be true if the spheroid was conductive, where a second term would appear in Eq. $(3.5)_2$ for the particle's conduction. The expression (3.6) holds true for the case of many spheroids identically oriented of a total volume $1-n$, as far as n represents very dilute dispersions. This is because the above equations are valid for many particles if the electric fields around each particle do not appreciably disturb each other. The effect of a dense mixture will be considered later.

3.2. The vertical formation factor F_v

In a sand sample not all particles are identically oriented. Here attention will be focused on a transversely isotropic sand sample, with the direction OV being the axis of rotational symmetry along the vertical direction of the sample. Figure 3b illustrates the three-dimensional model reflecting the transversely isotropic symmetries. The long axis OA of a particle forms an angle θ with OV. Since rotational symmetry around OV is established by thin section studies, the position of OA is not fixed as OA may conceivably rotate around OV keeping θ constant with equal probability to occupy any such position. Statistically, however, it is equivalent to consider OA on a vertical plane VOS which forms equal angles of 45° with two other vertical planes VOH_1 and VOH_2; the OH_1 and OH_2 are two arbitrarily chosen perpendicular to each other horizontal directions forming with OV a Cartesian coordinate system. Then a probability density function

$p(\theta)$ characterizes the distribution of long axes' orientation with respect to OV for $0 \leqslant \theta \leqslant \pi/2$, such that

$$\int_0^{\pi/2} p(\theta)d\theta = 1. \tag{3.7}$$

Using Eqs. (3.2), (3.6), and (3.7) and considering θ as a random variable, the expected value of the formation factor F_v along the vertical direction is obtained by

$$F_v = \int_0^{\pi/2} p(\theta)F_\theta d\theta = 1+\frac{1-n}{n}f_v, \tag{3.8}$$

where f_v is called the vertical form factor given by

$$f_v = \frac{2S-P_\theta(3S-1)}{2S(1-S)} \tag{3.9}$$

and P_θ is called the orientation factor obtained from

$$P_\theta = \int_0^{\pi/2} p(\theta)\cos^2\theta\, d\theta. \tag{3.10}$$

FRICKE [6] has derived a similar expression to Eq. (3.8) but the f_p was a function of particles' shape only, thus precluding dependence of F on the direction of measurement.

3.3. The horizontal formation factor F_h

The long axis OA forms an angle ω with OH_1 or OH_2, Fig. 3b, which varies from $\pi/2$ to $\pi/4$ as θ changes from 0 to $\pi/2$, and is related to θ by $\cos^2\theta+2\cos^2\omega = 1$. A corresponding probability density function $p(\omega)$ determines the statistical orientation of the particles with respect to the horizontal direction OH_1 or OH_2. The $p(\omega)$ must be related to $p(\theta)$ in such a way that the same number of particles exists at corresponding angular intervals $d\omega$ and $d\theta$, i.e. $p(\omega)d\omega = -p(\theta)d\theta$ where the minus sign indicates the decrease of ω with increasing θ. Using the above, a horizontal orientation factor P_ω can be defined and related to P_θ by

$$P_\omega = \int_{\pi/2}^{\pi/4} p(\omega)\cos^2\omega d\omega = \frac{1}{2}\int_0^{\pi/2} p(\theta)\,(1-\cos^2\theta)d\theta = \frac{1}{2}(1-P_\theta). \tag{3.11}$$

The horizontal formation and form factors F_h and f_h are obtained by expressions identical to Eqs. (3.8) and (3.9) substituting P_ω for P_θ; using Eq. (3.11) this yields

$$F_h = 1+\frac{1-n}{n}f_h, \tag{3.12}$$

$$f_h = \frac{S+1+P_\theta(3S-1)}{4S(1-S)}. \tag{3.13}$$

3.4. Particular cases

It is interesting to examine some particular cases. For spherical particles $R = 1$ and Eqs. (3.3) or (3.4) yield $S = 1/3$. Then Eqs. (3.9) and (3.13) yield $f_v = f_h = 3/2$ and Eqs. (3.8) and (3.12) yield $F_v = F_h = (3-n)/2n$ which is the Maxwell's expression for a dilute dispersion of non-conductive spheres [7]. On the other extreme, for long infinite cylinders $R = 0$ and Eq. (3.3) yields $S = 1/2$. If the cylinders are parallel to the vertical direction, the formation factor measured in a direction perpendicular to the cylinder's axes is the F_h given by Eqs. (3.12) and (3.13) for $P_\theta = 1$, since in that case $\cos\theta = 1$; for $S = 1/2$ and $P_\theta = 1$, Eqs. (3.13) and (3.12) yield $f_h = 2$ and $F_h = (2-n)/n$, retrieving an expression derived by RAYLEIGH [15] for infinite long non-conductive parallel cylinders in a dilute dispersion. Finally, laminae-shaped particles are obtained for $R \to \infty$ for which Eq. (3.4) yields $S \to 0$; then with $P_\theta = 0$ for F_v or $P_\theta = 1$ for F_h which implies electrical measurement parallel to the laminae planes, Eqs. (3.8), (3.9), (3.12), and (3.13) yield $f_v = f_h = 1$ and $F_v = F_h = 1/n$. For all other orientations the above equations yield $f_v = f_h = F_v = F_h = \infty$ as expected for thin laminae totally blocking the passage of electric current under any inclination. The above results were obtained by WIENER [19], although the case of the infinite values was obtained only for laminae-oriented normal to the direction of electrical measurement.

4. The effect of concentration

Equations (3.8) and (3.12) are rigorously valid for high porosities since their derivation requires that the surrounding fields of adjacent particles do not perturb each other appreciably. For sands, even at the loosest state the porosity is low enough to invalidate such an assumption. An exact mathematical treatment of field interaction is impossible. Indirect approximation methods must be considered, and the most widely accepted is Bruggeman's integration technique [4] for spheres, which was extended to randomly oriented ellipsoids by MEREDITH [8] and will be applied here for the case of transversely isotropic sands as follows. The mixture with real porosity n is considered as a continuum of fictitious porosity $\bar{n} = 1$ and conductivity $k_m + dk_m$ from the point of view of an additional fraction of solid particles. This additional fraction reduces the conductivity to k_m and changes the porosity by $d\bar{n} = dn/n$ as it can be easily proved. With dn very small, an expansion of Eq. (3.8) in Taylor series around $\bar{n} = 1$ with only the linear terms in $d\bar{n}$ (or dn) yields

$$F_v(1-d\bar{n}) = \frac{k_m+dk_m}{k_m} = 1+f_v\frac{dn}{n}. \tag{4.1}$$

Integrating Eq. (4.1) from k_e to k_m and from 1 to n with the initial condition $F_v = 1$ for $n = 1$, follows

$$F_v = n^{-f_v}. \tag{4.2}$$

In a similar way, Eq. (3.12) yields

$$F_h = n^{-f_h}, \tag{4.3}$$

where f_v and f_h are given by Eqs. (3.9) and (3.13). It is worth mentioning that during the integration process f_v and f_h were assumed constants implying from Eqs. (3.9) and (3.13) that P_θ did not change, which can be debated on the grounds that change of porosity may change the orientation. It must be remembered however, that the application of Bruggeman's technique of progressively decreasing the porosity is a fictitious one, serving only to reach the final porosity with the corresponding orientation, taking into account indirectly the field interaction. This must be contrasted to a real change of porosity through deformation for example, which will alter P_θ by reorientation of particles. Finally, the anisotropy index $A = (F_v/F_h)^{\frac{1}{2}}$ introduced by ARULANANDAN and KUTTER [3] can be easily obtained from Eqs. (3.9), (3.13), (4.2), and (4.3)

$$A = \left(\frac{F_v}{F_h}\right)^{\frac{1}{2}} = n^a, \quad a = \frac{(3S-1)(3P_\theta-1)}{8S(1-S)}, \tag{4.4}$$

where a is called the anisotropy factor.

Isotropic sands are characterized by a random orientation of particles which implies equal angles of the long axis with the three coordinate axes OV, OH_1, and OH_2. This yields $\cos^2\theta = 1/3$, and from Eqs. (3.7) and (3.10) $P_\theta = 1/3$. Then, from Eqs. (3.9), (3.13), (4.2), and (4.3) it can be easily derived that $F_v = F_h = F$, $f_v = f_h = f$ where

$$F = n^{-f}, \quad f = \frac{3S-1}{6S(1-S)}. \tag{4.5}$$

5. Discussion

5.1. The effect of orientation on F

The change of F_v and F_h with porosity for different values of P_θ as predicted by Eqs. (3.9), (3.13), (4.2), and (4.3) are illustrated by the curves of Fig. 4 which correspond to either F_v or F_h and in some cases to both of them, e.g. when $P_\theta = 1/3$ (isotropy). The corresponding values of P_θ are shown at the left side of the figure for F_v and the right side for F_h. The value $R = 0.65$ which yields from Eq. (3.3) $S = 0.386$ was chosen to correspond to the shape of particles for Monterey '0' sand, as will be discussed later in detail. The values $P_\theta = 0$ and $P_\theta = 1$ imply horizontal and vertical placement of the semiaxis a, respectively. Observe that for a given porosity F_v decreases and F_h increases with increasing P_θ which can be interpreted as follows. Recalling the definition of P_θ, (Eq. (3.10)), increasing P_θ implies an increase of the vertical orientation of the particles; this presents to the electric current along the vertical a smaller non-conductive target area, therefore the electric path which follows the contours of the particles becomes less tortuous and consequently the vertical conductivity of the mixture increases. This yields a decrease of F_v. Similar arguments show that F_h must increase with P_θ.

It is convenient to interpret P_θ in terms of an average azimuthal angle $\bar{\theta}$ defined from $\bar{\theta} = \cos^{-1}\sqrt{P_\theta}$, consistent with the definition of P_θ. For $P_\theta < 1/3$ and $\bar{\theta} > 54.74°$, $F_v > F_h$ and for $P_\theta > 1/3$, $\bar{\theta} < 54.74°$, $F_v < F_h$. Experimentally measured values of F_v for different methods of preparation of Monterey '0' sand samples at different porosities are

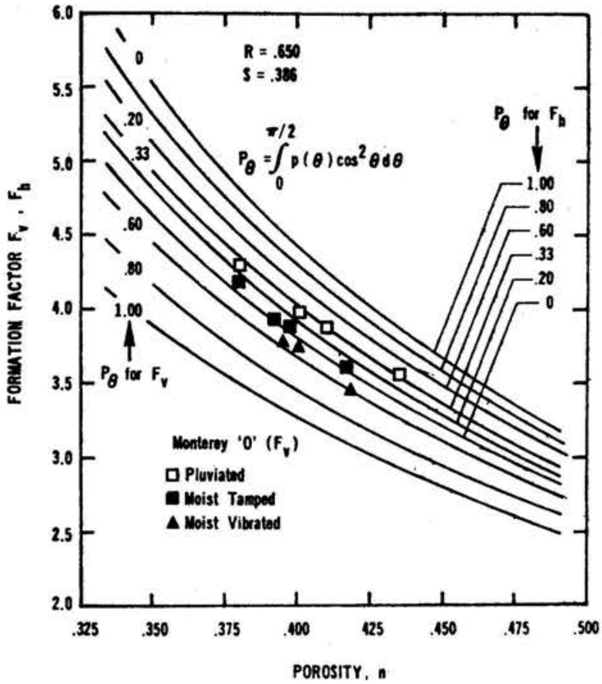

FIG. 4. Change of the vertical and horizontal formation factors with porosity for different orientation factors.

plotted on top of the theoretical curves in Fig. 4. In view of the above discussion, these values show that the tendency for horizontal orientation increases from moist vibrated to moist tamped to dry pluviated samples, with the pluviated sand being closer to random orientation (closer to the curve with $P_\theta = 1/3$). MITCHELL *et al.* [11] have reached the same conclusion as far as the relative orientation of the different samples is concerned by thin sections studies, but it was stated that the moist vibrated sample was closer to random orientation. This apparent difference stems from the two-dimensional interpretation of the obtained histograms, Figs. 1 and 2, while here a three-dimensional interpretation is incorporated in the derived relations and later used in connection with the histograms. Observe finally that no great change of P_θ occurs as porosity changes, since the experimental points lie approximately on the same theoretical curve.

5.2. Bounds on the values of form and anisotropy factors

For a given axial ratio R the values of the form and anisotropy factors f_v, f_h, and a vary with P_θ. Upper and lower bounds on these variations can be established easily for all R recalling that $0 \leqslant P_\theta \leqslant 1$. The results are shown by the curves of Fig. 5 for f_v, f_h, and the upper part of Fig. 6 for a. For each axial ratio R, S was computed from Eqs. (3.3) or (3.4) and f_v, f_h, and a were computed from Eqs. (3.9), (3.13), and (4.4) for different P_θ. The curves for $P_\theta = 0$ and $P_\theta = 1$ are the upper and lower bounds, restricting the values of f_v, f_h, and a within the space of the "fan" created by the different curves.

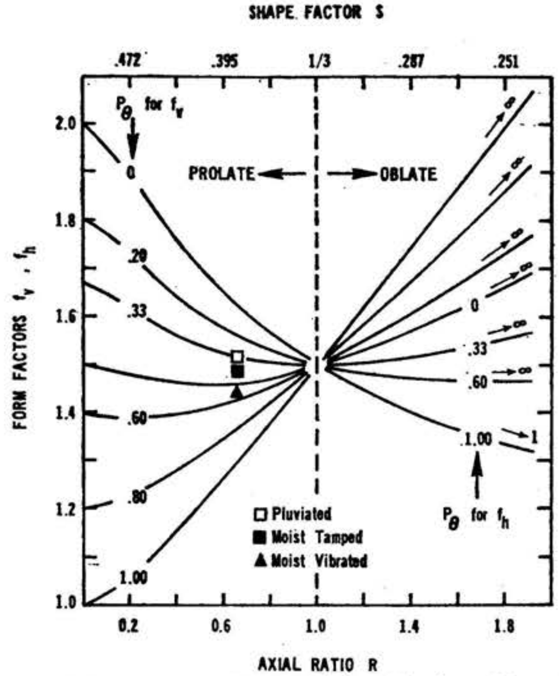

FIG. 5. Change and upper and lower bounds of the vertical and horizontal form factors with axial ratio for different orientation factors.

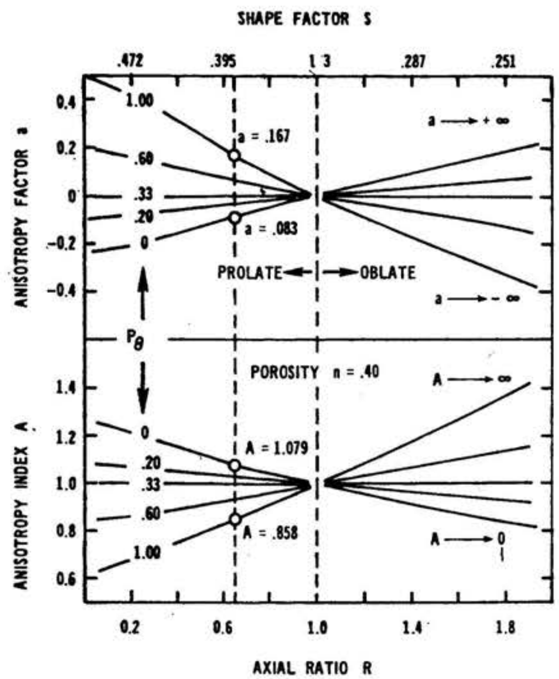

FIG. 6. Change and upper and lower bounds of the anisotropy factor and the anisotropy index (for $n = 0.40$) with axial ratio for different orientation factors.

For $R = 1$, $S = 1/3$, $f_v = f_h = f = 1.5$ for all P_θ which in combination with Eq. (4.5) retrieves Bruggeman's expression for non-conductive spheres [14]. Also for $R = 1$, $a = 0$ yielding $A = 1$; the latter is also true for any R and $P_\theta = 1/3$ (isotropy). The possible range of values for f_v, f_h and a for all P_θ decreases as $R \to 1$ (apex of the "fan"). For infinite long cylinders $R = 0$, $S = 0.500$ and $1 \leqslant f_v \leqslant 2$, $1.5 \leqslant f_h \leqslant 2$, $-0.25 \leqslant a \leqslant 0.500$. Thus, it can be safely said that no value of f can be less than 1 or greater than 2 for any $R \leqslant 1$. Experimentally determined values of $f_v = -\log F_v/\log n$, Eq. (4.2), are plotted in Fig. 5 for $R = 0.65$ falling within the accepted "fan" space. As $R \to \infty$ (laminae), the limits of f_v, f_h and a are clearly indicated for different P_θ, and the reader is referred to a previous section for particular cases. It is interesting to note that as $R \to \infty$, $a \to \infty$ for $P_\theta < 1/3$ and $a \to -\infty$ for $P_\theta > 1/3$. In the lower part of Fig. 6 the corresponding variations of the anisotropy index $A = n^a$ with R and P_θ are shown for $n = 0.40$, together with the bounds and the different limiting values; for example, for $R = 0.65$ the values of a must fall in the range $-0.083 \leqslant a \leqslant 0.167$ from Eq. (4.4) and P_θ equal to 0 and 1 respectively, which yields $0.858 \leqslant A \leqslant 1.079$.

6. Prediction of the formation factors using thin sections studies

6.1. Method

In this section the values of F_v, F_h and A will be predicted from the corresponding formulas and compared with experimentally measured values. The experimental methods and equipment used to measure the formation factors F_v, F_h are reported in detail in [3]. It suffices to say here that great attention was given to saturate fully the used samples applying back pressure whenever necessary, since the degree of saturation has an important effect in electrical measurements of conductivity. It is apparent that two pieces of information are necessary for the prediction: the shape factor S and the orientation factor P_θ. The former will be obtained from Eq. (3.3) once the axial ratio R is known, and the latter from Eq. (3.10) in combination with thin sections studies.

6.2. The shape factor S

Since thin sections studies are available for Monterey '0' sand, this sand will be the object of the investigation. Monterey '0' is a uniform, sub-rounded sand consisting predominantly of quartz with some feldspar and mica. A quartz grain has in general a major, intermediate and minor axes denoted by a, b, c respectively and can be modelled by an ellipsoid of corresponding dimensions. A grain shape histogram of particles' length to width ratios was obtained by direct observation of grains lying on a horizontal plane. Naturally the grains rested on their most stable position presenting their intermediate and long axes to the observer. The average ratio $R_1 = (b/a)$ of those axes was found equal to 0.72 [11]. For a proper modelling of sand particles as prolate spheroids, an estimation of the ratio $R_2 = (c/a)$ is also necessary. This can be achieved by using the formulas suggested by WADELL [17, 18] in order to obtain the sphericity ψ of a quartz particle, namely $\psi = (d_c/D_c) = (d_n/D_s)+0.1$. Here, d_c is the diameter of a circle equal in area to the area obtained when the grain rests on a face parallel to the plane of the long and intermediate axes, D_c is the diameter of the smallest circle circumscribing this face, d_n denotes the diameter of a sphere with the same volume as the particle and D_s represents the diameter of the smallest sphere circumscribing the particle. Interpreting the above quantities in terms of R_1, R_2 allows us to write

$$\psi = \sqrt{R_1} = \sqrt[3]{R_1 R_2}+0.1. \tag{6.1}$$

With $R_1 = 0.72$ Eq. (6.1) yields $R_2 = 0.58$. Modelling now the grain as a prolate spheroid $a > b = c$, the axial ratio $R = b/a$ is taken as the geometric mean of R_1' and R_2 so that the area of the ellipse with the axes b and c is preserved, i.e. $R = \sqrt{R_1 R_2} = 0.65$ for which Eq. (3.3) yields $S = 0.386$ as already mentioned.

6.3. The orientation factor P_θ

The P_θ can be obtained from Eq. (3.10) if the probability density $p(\theta)$ is known. The $p(\theta)$ is given in a discrete form as the percent frequency p_θ of the long axes orientation with respect to the vertical obtained by the histograms of Figs. 1 and 2, where the sum of p_θ from $\theta = 0°$ to $\theta = 180°$ is equal to one. Noting that $\cos^2\theta = \cos^2(\pi-\theta)$, Eq. (3.10) can be written in a discrete form as

$$P_\theta = \sum_{\theta=5°}^{\theta=85°} (p_\theta+p_{\pi-\theta})\cos^2\theta, \tag{6.2}$$

Table 1. Tabulation of the per cent frequency of long axes orientation from the histograms of Figs. 1 and 2 and calculation of the orientation factor and average azimuthal angle.

	Per cent frequency of long axes orientation $p_\theta+p_{\pi-\theta}$				
	Porosity $n = 0.380$		Porosity $n = 0.419$		
Azimuthal angle θ (1)	Dry pluviated (2)	Moist tamped (3)	Dry pluviated (4)	Moist tamped (5)	Moist vibrated (6)
5°	5.20	7.70	5.00	8.90	9.20
15°	5.30	6.90	5.00	7.20	8.60
25°	6.80	9.00	11.00	7.70	8.20
35°	6.40	11.80	13.80	11.20	9.00
45°	10.40	14.00	12.00	9.30	11.00
55°	15.20	10.80	9.20	11.60	14.80
65°	17.20	15.80	17.60	16.60	10.00
75°	16.80	14.20	13.60	12.70	17.60
85°	16.70	9.80	12.40	14.80	11.60
Orientation factor $P_\theta = \sum_{\theta=5°}^{\theta=85°} (p_\theta+p_{\pi-\theta})\cos^2\theta$ and $\bar{\theta} = \cos^{-1}\sqrt{P_\theta}$					
P_θ	0.340	0.438	0.414	0.420	0.434
$\bar{\theta}$	54.33°	48.56°	49.95°	49.60°	48.79°

where summation is carried out for nine 10° angular intervals from 0° to 90°, taking θ at the middle of each interval, i.e. $\theta = 5°, 15°, \ldots, 85°$. The values of $p_\theta + p_{\pi-\theta}$ from the histograms and the computed values of P_θ from Eq. (6.2) as well as the average azimuthal angles $\bar{\theta} = \cos^{-1}\sqrt{P_\theta}$ are tabulated in Table 1. The values of P_θ, and more clearly of $\bar{\theta}$, show that pluviation tends to orient the particles more towards the horizontal than the method of moist tamping and moist vibration. This was observed directly from the measured values of F_v, Fig. 4. Also, decrease in porosity from 0.419 to 0.380 renders the pluviated particles more horizontal by 4.50° and the vibrated particles more vertical by 1° if $\bar{\theta}$ is used as a measure.

6.4. Comparison with experiments

Using $S = 0.386$ and the values of P_θ from Table 1, the values of f_v, f_h, a and of F_v, F_h, A can be predicted from Eqs. (3.9), (3.13), (4.2), (4.3), and (4.4), and are tabulated in columns 4 and 5 respectively of Tables 2, 3, and 4. The experimentally measured values are shown in columns 6 of the above tables. For the moist tamped sample at $n = 0.397$ no corresponding histogram was available, thus P_θ was obtained by interpolation be-

Table 2. Prediction of the vertical formation factor using the orientation factor calculated from thin sections studies and comparison with measured walues.

Monterey '0' preparation method (1)	Porosity n (2)	Orientation factor P_θ (3)	Vertical form factor Equation (3.9) f_v (4)	Vertical formation factor $F_v = n^{-f_v}$ (5)	Vertical formation factor measured (6)	Per cent error % (7)
Dry	0.380	0.340	1.515	4.33	4.32	0.23
Pluviated	0.419	0.414	1.491	3.66	3.74	−2.14
Moist	0.380	0.438	1.483	4.20	4.22	−0.47
Tamped	0.397	0.429	1.486	3.94	3.92	0.51
	0.419	0.420	1.488	3.64	3.60	−1.11
Moist Vibrated	0.419	0.434	1.484	3.63	3.47	4.60

Table 3. Prediction of the horizontal formation factor using the orientation factor calculated from thin sections studies and comparison with measured values.

Monterey '0' preparation method (1)	Porosity n (2)	Orientation factor P_θ (3)	Horizontal form factor Eq. (3.13) f_h (4)	Horizontal formation factor $F_h = n^{-f_h}$ (5)	Horizontal formation factor measured (6)	Per cent error % (7)
Pluviated	0.380	0.340	1.518	4.34	4.18	3.83
M. Tamped	0.397	0.429	1.533	4.12	3.97	3.78
M. Vibrated	0.419	0.434	1.534	3.80	3.60	5.56

Table 4. Prediction of the anisotropy index using the orientation factor calculated from thin sections studies and comparison with measured values.

Monterey '0' preparation method (1)	Porosity n (2)	Orientation factor P_θ (3)	Anisotropy form factor Eq. (4.4) a (4)	Anisotropy index $A = n^a$ (5)	Anisotropy index A measured (6)	Per cent error % (7)
Pluviated	0.380	0.340	0.0017	0.998	1.016	−1.77
M. Tamped	0.397	0.429	0.0239	0.978	0.994	−1.60
M. Vibrated	0.419	0.434	0.0252	0.978	0.982	−0.41

tween the P_θ at $n = 0.38$ and $n = 0.419$. As the percent errors show in columns 7, the agreement between measured and predicted values is very satisfactory for most cases.

The agreement is much better for F_v than for F_h. This can be attributed to two factors: first, the P_θ is computed directly from vertical thin sections histograms and its use to predict F_h assumes ideal transversely isotropic symmetries which may not be satisfied; second, the values of F_h were measured initially in cubical samples and then corrected by a geometrical factor to correspond to measurements of F_v in cylindrical samples [3]; this may have introduced some error for F_h.

7. Summary and conclusions

The electric conductivity of sand samples saturated by water assumes different values if measured along different directions as a result of particles' orientation within the samples. This property renders the formation factor F a direction-dependent index of the sand structure, especially suited to characterize mechanical sand anisotropy which is also the result of particles orientation. This has been used recently to correlate F to sand liquefaction behavior [3]. It was possible to develop theoretically, on the basis of the electromagnetic theory, analytical relations between F, the porosity and parameters associated with the shape and orientation of particles for transversely isotropic sands and establish theoretical upper and lower bounds on those parameters. Obtaining the values of the shape and orientation parameters independently from thin sections studies, the theoretically predicted values of F along the axes of transverse isotropy were in close agreement with experimentally measured values. This gave a sound theoretical confirmation of the experimentally known fact that F depends on the sand structure, especially on the orientation of the particles which cannot be accounted by other indices like relative density.

One point, however, should be discussed further. In the theoretical development no explicit parameter accounted for the size and size distribution of the particles, because the fundamental work of Maxwell and Fricke, an extension of which is the present work, proved that only the shape is important for the solution of the Laplace equation for the potential. This is true as far as the size of a particle remains sufficiently small compared to the dimensions of the electrolyte cell in order to eliminate wall effects, and sufficiently large to eliminate the effect of surface resistance, however small for sands, which depends on the size (for clays, for example, this must be considered). This is true for very dilute dispersions for which Maxwell's equation is valid. When the porosity decreases, the electric fields around the particles begin to interact and this was taken into account indirectly by applying Bruggeman's technique. Still, there is no reason to assume that the size as such should have any effect on the field interaction. The size distribution, however, i.e. the gradation, may have an effect on the field interaction which does not reflect on the Bruggeman's technique by its very nature, thus no parameter associated with gradation appears explicitly in the theory. Well-graded sand will attain lower porosities than uniform one, and this increases the values of F, but the question remains if different gradation effects F at the same porosity. Experiments performed by DE LA RUE and TOBIAS [5] and MEREDITH and TOBIAS [9] on single and mixed size spherical particles showed very small differences on the values of the formation factor. For non-spherical particles perhaps the difference is greater (if shape effects is coupled with gradation) and more experiments are necessary in order to draw sharp conclusions.

In the present development uniform sands (like Monterey '0') were considered, therefore gradation was not important. If further work proves that gradation does not appreciably affect the formation factor, then, since some mechanical properties depend on gradation, it will be necessary to combine the formation factor with some other index for a proper correlation with those mechanical properties. In fact, this was done by ARULANANDAN and KUTTER [3] where the anisotropy index A was combined with relative density for the correlation with the liquefaction behavior of sands. Further work is under way so as to obtain correlation of the formation factors (vertical and horizontal) with other mechanical properties of anisotropic sands. Extension to anisotropic clays is feasible, but the basis equations must change appropriately since the clay particles are in general conductors.

Acknowledgements

The authors wish to acknowledge partial support of this research by the National Science Foundation Grant ENG 76-13146. They also wish to acknowledge Professor MITCHELL, *et al.* [11], for making available to them the report to U.S. Army Engineers Waterways Experiment Station on thin sections studies used in the present paper.

References

1. G. E. ARCHIE, *The electrical resistivity log as an aid in determining some reservoir characteristics*, Tran AIME, **146**, 54–61, 1942.
2. J. R. F. ARTHUR and B. K. MENZIES, *Inherent anisotropy in sand*, Geotech., **22**, 1, 115–128, 1972.
3. K. ARULANANDAN and B. KUTTER, *A directional structure index related to sand liquefaction*, Proc. ASCE, Geotechnical Engineering Division Speciality Conference, Earthquake Engng. Soil Dynamics, **1**, 213–230, 1978.
4. D. A. G. BRUGGEMAN, *Berechnung verschiedenez physikalischer Konstanten von beterogenen Substanzen*, Ann. Phys. Lpz., **24**, 5, 636, 1935.

5. R. E. DE LA RUE and C. W. TOBIAS, *On the conductivity of dispersions*, J. Electrochem. Soc., **106**, 9, 827–833, 1959.
6. H. FRICKE, *A mathematical treatment of the electric conductivity and capacity of disperse systems*, Phys. Rev., **24**, 575–587, 1924.
7. J. C. MAXWELL, *A treatise on electricity and magnetism*, Oxford Univ. Press, London 1892.
8. R. E. MEREDITH, *Studies on the conduction of dispersions*, Thesis, University of California, Lawrence Radiation Laboratory, UCRL-8667, Berkeley 1959.
9. R. E. MEREDITH and C. W. TOBIAS, *Conductivities in emulsions*, J. Electrochem. Soc., **108**, 3, 286–290, 1961.
10. R. E. MEREDITH and C. W. TOBIAS, *Conduction in heterogeneous systems*, Adv. Electrochem. Electrochem. Engng., 2, ed. by C. W. TOBIAS, J. Wiley and Sons Inc., New York 1962.
11. J. K. MITCHELL, J. M. CHATOIAN and G. C. CARPENTER, *The influence of fabric in the liquefaction behaviour of sand*, Report to U.S. Army Engineering Waterways Experiment Station, Vicksburg, Berkeley 1976.
12. M. ODA, *Initial fabrics and their relation to mechanical properties of granular materials*, Soils and Foundations, **12**, 1, 17–37, 1972.
13. M. ODA, *The mechanism of fabric changes during compression deformation of sands*, Soil and Foundations, **12**, 2, 1–18, 1972.
14. M. ODA, *Deformation mechanism of sand in triaxial compression tests*, Soils and Foundations, **12**, 4, 45–63, 1972.
15. RAYLEIGH, lord (J. W. STRUTT), *On the influence of obstacles arranged in rectangular order upon the properties of a medium*, Phil. Mag., **34**, 481–502, 1892.
16. J. A. STRATTON, *Electromagnetic theory*, McGraw-Hill, New York 1941.
17. H. WADELL, *Shape determination of large cedimental rock-fragments*, Pan-American Geologist, Des Moines, **61**, 187–220, 1934.
18. H. WADELL, *Volume, shape and roundness of quartz particles*, J. Geol., **43**, 250–280, 1935.
19. O. WIENER, *Abhandl. sächs. Ges. Wiss.*, Math.-Phys., **32**, 509, 1912.
20. M. R. J. WYLLIE and A. R. GREGORY, *Formation factors of unconsolidated porous media: influence of particle shape and effect of sementation*, Petroleum Trans., AIME, **198**, 103–110, 1953.
21. J. P. BOEHLER and A. SAWCZUK, *Analyse geometric des criteres d'ecoulement plastique anisotrope*, Problemes de Rheologie, Symp. franco-polonais de rheologie, Nice 1974.
22. J. P. BOEHLER and A. SAWCZUK, *On yielding of oriented solids*, Acta Mech., **27**, 185–206, 1977.
23. K. ARULANANDAN and Y. F. DAFALIAS, *Significance of formation factor in sand structure characterization*, Lett. Appl. Engng. Sci., **17**, 109–112, 1979.
24. Y. F. DAFALIAS and K. ARULANANDAN, *The structure of anisotropic sands in relation to electrical measurements*, Mechanics Research Communications, **5**, 325–330, 1978.

DEPARTMENT OF CIVIL ENGINEERING
UNIVERSITY OF CALIFORNIA, DAVIS, USA.

Received August 19, 1978.